Cellular/Molecular

Functional Characterization of 5-HT$_{1B}$ Receptor Drugs in Nonhuman Primates Using Simultaneous PET-MR

Hanne D. Hansen,[1] Joseph B. Mandeville,[2] Christin Y. Sander,[2] Jacob M. Hooker,[2] Ciprian Catana,[2] Bruce R. Rosen,[2] and Gitte M. Knudsen[1,3]

[1]Neurobiology Research Unit and NeuroPharm, Copenhagen University Hospital (Rigshospitalet), 2100 Copenhagen, Denmark, [2]MGH/HST A. A. Martinos Center for Biomedical Imaging, Massachusetts General Hospital, Charlestown, Massachusetts 02129, and [3]Faculty of Health and Medical Sciences, University of Copenhagen, 2200 Copenhagen, Denmark

In the present study, we used a simultaneous PET-MR experimental design to investigate the effects of functionally different compounds (agonist, partial agonist, and antagonist) on 5-HT$_{1B}$ receptor (5-HT$_{1B}$R) occupancy and the associated hemodynamic responses. In anesthetized male nonhuman primates ($n = 3$), we used positron emission tomography (PET) imaging with the radioligand [^{11}C]AZ10419369 administered as a bolus followed by constant infusion to measure changes in 5-HT$_{1B}$R occupancy. Simultaneously, we measured changes in cerebral blood volume (CBV) as a proxy of drug effects on neuronal activity. The 5-HT$_{1B}$R partial agonist AZ10419369 elicited a dose-dependent biphasic hemodynamic response that was related to the 5-HT$_{1B}$R occupancy. The magnitude of the response was spatially overlapping with high cerebral 5-HT$_{1B}$R densities. High doses of AZ10419369 exerted an extracranial tissue vasoconstriction that was comparable to the less blood–brain barrier-permeable 5-HT$_{1B}$R agonist sumatriptan. By contrast, injection of the antagonist GR127935 did not elicit significant hemodynamic responses, even at a 5-HT$_{1B}$R cerebral occupancy similar to the one obtained with a high dose of AZ10419369. Given the knowledge we have of the 5-HT$_{1B}$R and its function and distribution in the brain, the hemodynamic response informs us about the functionality of the given drug: changes in CBV are only produced when the receptor is stimulated by the partial agonist AZ10419369 and not by the antagonist GR127935, consistent with low basal occupancy by endogenous serotonin.

Key words: 5-HT$_{1B}$; nonhuman primates; PET-MR imaging; pharmacology

Significance Statement

We here show that combined simultaneous positron emission tomography and magnetic resonance imaging uniquely enables the assessment of CNS active compounds. We conducted a series of pharmacological interventions to interrogate 5-HT$_{1B}$ receptor binding and function and determined blood–brain barrier passage of drugs and demonstrate target involvement. Importantly, we show how the spatial and temporal effects on brain hemodynamics provide information about pharmacologically driven downstream CNS drug effects; the brain hemodynamic response shows characteristic dose-related effects that differ depending on agonistic or antagonistic drug characteristics and on local 5-HT$_{1B}$ receptor density. The technique lends itself to a comprehensive *in vivo* investigation and understanding of drugs' effects in the brain.

Introduction

Development of novel drugs is complex, costly, and time-consuming and this particularly applies to drugs targeting the CNS, where the time-to-market is ~20% longer than for non-CNS drugs (Lindsley, 2014). The process is also risky: only 6.2% of the drugs entering clinical trials obtain clinical approval (Lindsley, 2014). Accordingly, it is of major importance to be able to reliably predict target involvement and to establish mechanisms of action and efficacies of novel drugs *in vivo* in humans. *In vitro* experi-

Received July 14, 2017; revised Aug. 24, 2017; accepted Sept. 22, 2017.

Author contributions: H.D.H., J.B.M., J.M.H., B.R.R., and G.M.K. designed research; H.D.H., J.B.M., C.Y.S., J.M.H., C.C., and G.M.K. performed research; C.C. contributed unpublished reagents/analytic tools; H.D.H., J.B.M., and C.Y.S. analyzed data; H.D.H., J.B.M., C.Y.S., J.M.H., C.C., B.R.R., and G.M.K. wrote the paper.

This work was supported by the Lundbeck Foundation, University of Copenhagen, Innovation Fund Denmark, and grants from the National Institute of Health (R90DA023427, P41EB015896, S10RR026666, S10RR022976, S10RR019933, S10RR017208). We thank the staff and technical personnel at the MGH/HST A. A. Martinos Center for Biomedical Imaging including Helen Deng, Grae Arabasz, Shirley Hsu, Regan Butterfield, Judit Sore, Samantha To, Steve Carlin, and Chris Moseley.

Conflict of interest: G.M.K. has been an invited lecturer at Pfizer A/S, worked as a consultant and received grants from H. Lundbeck A/S and is a stock holder of Novo Nordisk/Novozymes. The remaining authors declare no competing financial interests.

Correspondence should be addressed to Dr. Hanne D. Hansen, Neurobiology Research Unit and NeuroPharm, Section 6931, Copenhagen University Hospital, Rigshospitalet, Blegdamsvej 9, 2100 Copenhagen, Denmark. E-mail: hanne.d.hansen@nru.dk.

DOI:10.1523/JNEUROSCI.1971-17.2017

 0270-6474/17/3710671-08$15.00/0

ments and the use of experimental animals provide important information about the drugs, but unfortunately, the experimental models often fail to predict the effects in humans. The closest preclinical models available are the nonhuman primates (NHPs), due to their similarity in physiology and anatomy to humans.

When used in conjunction with specific radioligands, PET critically informs about cerebral target involvement of novel drugs as well as their dose-dependent target occupancy. Likewise, pharmacological MRI (phMRI) investigates the functional brain response to a pharmacological intervention, demonstrating drug effects on the brain hemodynamics, usually interpreted as a downstream effect of changes in drug binding to its target (Jenkins, 2012). PET plays a well established role in Phase 1 studies to identify the clinical dose range to be used in the subsequent clinical trials (Matthews et al., 2012), and phMRI represents a potentially powerful tool in drug discovery, providing real-time neurophysiological data on drug action (Bourke and Wall, 2015). The recently established possibility to conduct multimodal and simultaneous imaging with PET-MRI (Catana et al., 2012) provides an exciting new research opportunity to study drug effects. Sander et al. (2013) described a model for the estimation of basal dopamine receptor occupancies, by administrating pharmacological doses of the D2/D3 receptor antagonist raclopride and measuring the neurovascular response simultaneous with the D2/D3 receptor occupancy. Further, simultaneous PET-fMRI enables characterization of dynamic neuroreceptor adaptations *in vivo*, and may offer a first noninvasive method for assessing receptor desensitization and internalization (Sander et al., 2016).

The aim of the current study was to demonstrate proof-of-concept that combined simultaneous PET-MRI informs about the mode of action within the brain, i.e., if the PET-MRI drug response reflects the pharmacological properties (agonist, antagonist), and blood–brain barrier (BBB) permeability of a given compound. For this purpose, we chose to examine drugs acting on a G-protein-coupled receptor, the 5-HT_{1B} receptor (5-HT_{1B}R). The 5-HT_{1B}Rs are involved in several psychophysiological functions and disorders: locomotor activity (Geyer, 1996), depression (Ruf and Bhagwagar, 2009), anxiety states, and aggressive-like behavior (da Cunha-Bang et al., 2017). Therapeutically, the 5-HT_{1B}R constitutes an important target in migraine intervention, where headache is alleviated by administration of triptans that mediate an agonist action on the 5-$HT_{1B/1D/1F}$ receptors resulting in vasoconstriction of the vessels (Elhusseiny and Hamel, 2001). It is still debatable exactly where the triptans exert their antimigraine effects: in the brain parenchyma, at the intravascularly located receptors, or through the nociceptive input from the trigeminal nerves (Schytz et al., 2017).

In this study, we investigated in anesthetized NHPs the pharmacological actions on the cerebral 5-HT_{1B}R occupancy and hemodynamics. We used PET-MR imaging with the PET radioligand [^{11}C]AZ10419369 administered as a bolus followed by constant infusion to measure changes in 5-HT_{1B}R occupancy. Simultaneously, we measured changes in CBV as a proxy of downstream drug effects on neuronal activity (Belliveau et al., 1991; Qiu et al., 2012). As pharmacological tools, we used three different drugs with specific pharmacological actions on the 5-HT_{1B}R: the partial agonist AZ10419369 (Maier et al., 2009), the agonist sumatriptan (Schoeffter and Hoyer, 1989), and the antagonist GR127935 (Skingle et al., 1996). Moreover, with the entire NHP head within the scanner field-of-view, we were able to simultaneously assess central effects on brain tissue and peripheral effects in extracranial tissue. Consistent with classical pharmacology, we hypothesized that 5-HT_{1B}R stimulation with a BBB-permeable agonist would initiate downstream signaling pathways associated with dose-dependent alterations in the hemodynamic response, whereas antagonists would have no effects on the hemodynamic response.

Table 1. Experimental details

Monkey	Weight, kg	Inj. mass, μg/kg	BP_{ND}	Drug	Drug dose, μg/kg	Time of administration, min	Induction anesthetics
M1	10.6	0.70	2.15	BSL	—	—	Type 1
M3	7.4	0.41	2.04	BSL	—	—	Type 1
M2	11.4	0.13	2.02	AZ	0.88	55.2	Type 1
M1	10.6	0.12	1.91	AZ	0.94	65.5	Type 1
M1	10.6	0.27	2.09	AZ	1.89	52.3	Type 1
M1	10.6	0.12	2.07	AZ	2.86	55.0	Type 1
M3	7.4	0.25	1.94	AZ	4.05	62.4	Type 1
M2	12.0	0.56	1.74	AZ	4.17	60.0	Type 2
M3	10.3	0.34	1.90	AZ	4.85	59.9	Type 2
M2	13.8	0.15	0.88	AZ	5.00	60.0	Type 2
M2	13.8	0.14	0.61	AZ	36.20	40.0	Type 2
				AZ	5.00	60.0	
M3	10.3	0.37	1.67	Sumatriptan	19.4	59.6	Type 2
M2	12.0	0.30	1.70	GR127935	200	60.0	Type 2
M3	12.2	0.42	1.12	GR127935	200	62.8	Type 2
M3	12.2	0.31	n.a.	GR127935	500	−14.0	Type 2
				AZ	5.00	60.1	

BP_{ND} represent the baseline nondisplaceable binding potential before a challenge. BSL indicates a baseline experiment, where no challenge was given. Time of administration of the drug is relative to the injection (inj.) of the radioligand. Induction of anesthesia was performed in two ways: Type 1: diazepam (0.4 mg/kg) + ketamine (20 mg/kg); Type 2: ketamine (10 mg/kg) + xylazine (0.5 mg/kg) following reversal of xylazine with yohimbine (0.11 mg/kg).

Materials and Methods

Animal procedures. Three male rhesus macaques with mean weight of 11.1 ± 1.8 kg were used for *in vivo* simultaneous fMRI/PET imaging. Anesthesia was induced with an intramuscular injection of either 20 mg/kg ketamine with 0.4 mg/mg diazepam or 10 mg/kg ketamine with 0.5 mg/kg xylazine followed by reversal of xylazine with yohimbine (0.11 mg/kg). In all cases induction was also accompanied with an intramuscular injection of atropine (0.05 mg/kg). Induction of anesthesia was performed ~100 min before the start of the PET scan. A catheter for injections was placed in the saphenous vein. During scans, anesthesia was maintained by isoflurane (0.8–1.5%, mixed with pure oxygen) through an intubation tube without ventilation. Physiological changes (blood pressure, pulse, end-tidal CO_2, and breathing rate) were monitored continuously throughout the experiment. The procedures complied with the regulations of the Subcommittee on Research Animal Care at Massachusetts General Hospital.

Experimental design. Our experimental design was of a successively nature, with the outcomes of PET-MR scans raising questions that we would subsequently design experiments to answer. The different pharmacological challenges were, when possible, replicated in a different animal. Details for each individual experiment is given in Table 1.

PET acquisition. [^{11}C]AZ10419369 was given as a bolus plus infusion scheme with K_{bol} ranging from 1.3–2.2 h^{-1} (1.5 ± 0.3, mean ± SD; n = 15). The injected dose was 507 ± 72.3 MBq (mean ± SD). The NHPs were subsequently scanned for 120 min in list-mode with a research-dedicated human PET/MR scanner, which consists of a 3 T MRI scanner (MAGNETOM Trio, Tim system; Siemens AG, Healthcare Sector) and an MR-compatible PET insert (BrainPET; Siemens AG, Healthcare Sector). AZ10419369 (0.88–36.2 μg/kg; n = 11), sumatriptan (19.4 μg/kg; n = 1), and GR127935 (200 μg/kg; n = 2), were given as intravenous bolus injections 58 ± 6.2 min (n = 14) after bolus injection of [^{11}C]AZ10419369. In a blocking experiment with GR127935 (500 μg/kg; n = 1), the drug was administered 14 min before injection of the radioligand.

List-mode PET data were reconstructed into dynamic frames of increasing length (25 × 60, 11 × 300, and 4 × 600 s) with the ordinary

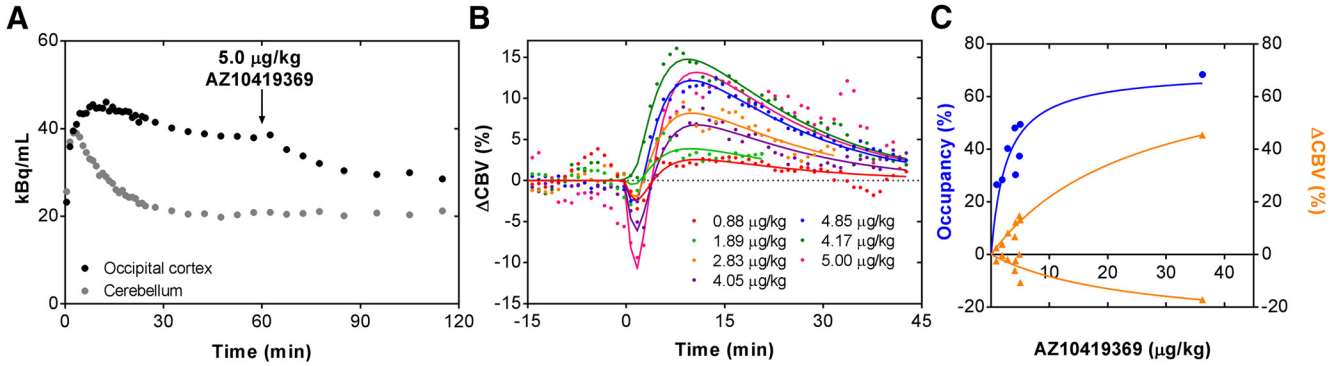

Figure 1. Dose–response relationship following AZ10419369 administration. ***A***, Representative time-activity curve of [^{11}C]AZ10419369 with the partial 5-HT$_{1B}$R agonist AZ10419369 (5.0 μg/kg) intravenously administrated 60 min after injection of the radioligand. ***B***, Percentage change in CBV [ΔCBV (%)] in the occipital cortex after intravenous injection of varying doses of AZ10419369. ***C***, Dose–response relationship of the 5-HT$_{1B}$R occupancy (blue) and the positive and negative peak relative change in CBV (orange).

Poisson expectation maximization algorithm with 32 iterations. After downsampling, the final reconstructed volume consisted of 76 slices with 128 × 128 pixels (2.5 mm isotropic voxels). Corrections for scattering and for attenuation of the head and the radiofrequency coil were applied during reconstruction (Catana et al., 2010).

fMRI acquisition. Dynamic functional MR scans (fMRI time series) were acquired using gradient-echo echoplanar imaging with whole-brain coverage. Before fMRI scanning, monocrystalline iron oxide nanocompound (Feraheme) was administered intravenously at 10 mg/kg to improve fMRI detection power (Mandeville, 2012). Two different receiver coils were used: a vendor-supplied circularly polarized local transmit birdcage coil with an eight-channel receive array and a custom-built eight-channel NHP receive array. We used echoplanar imaging with whole-brain coverage and an isotropic resolution of 1.3 mm (MR field-of-view = 110 × 72.8 mm2, bandwidth = 1350 Hz/pixel) with a temporal resolution of 3 s and echo time of 23 ms.

fMRI and PET data analysis. PET and MR data were preprocessed (coregistration, motion correction, spatial smoothing, definition of regions-of-interest,) as previously described (Sander et al., 2016) and statistical analysis was performed using the general linear model (GLM). The extracranial region was defined using the T1-weighted image to define a region in muscle outside the cranium. All fMRI data analysis and the voxel-based analysis in Figure 2 was performed with open-access software (www.nitrc.org/projects/jip).

Temporal responses to drug injections were modeled with gamma variate functions, in which times to peak and times to baseline were adjusted to minimize the χ^2/DOF of the GLM fit to the data:

$$f(t) = x^{\alpha} \cdot e^{\alpha \cdot (1-x)} \text{ where } x = \frac{t - t_0}{\tau},$$

$$\tau = 7.5\ min \text{ and } \alpha = 0.6\ min.$$

The resulting signal models were standardized for each drug, and results were converted to percentage change in CBV by standard methods (Mandeville et al., 1998) and subsequently adjusted for decreases in the animals' 5-HT$_{1B}$R availability due to aging (Nord et al., 2014).

Quantification of [^{11}C]AZ10419369 binding was performed as a region-based analysis with the extended simplified reference tissue model using the cerebellum gray matter (excluding the vermis) as reference region (Zhou et al., 2006). All graphical figures and correlations were created in GraphPad v6.04. All nonlinear regression assuming Mikaelis–Menten kinetics.

Results

Dose–response effects of the 5-HT$_{1B}$R partial agonist AZ10419469 on the PET-MRI signal

First, we assessed the dose–response effects of the 5-HT$_{1B}$R partial agonist AZ10419369. Consistent with the high BBB permeability of ^{11}C-labeled AZ10419369, we observed a time-dependent (Fig. 1*A*) and dose-dependent (Fig. 1*C*) increase in the cerebral 5-HT$_{1B}$R occupancy when AZ10419369 was injected intravenously as a within-scan challenge 57 ± 7.4 min (n = 9) after the injection of [^{11}C]AZ10419369. Within the tested dose-range (0.88–36.2 μg/kg), 5-HT$_{1B}$R occupancy in the occipital cortex was between 26.5 and 68.5% (Fig. 1*C*).

Intravenous injection of AZ10419369 induced a biphasic CBV response in the brain, with a rapid initial decrease followed by an increase that slowly returned to baseline values (Fig. 1*B*). A dose-dependent hemodynamic response was observed for decreases and increases of CBV, and this dose dependency was generally found throughout the brain. All data could be described by a nonlinear fit assuming Micheaelis–Menten kinetics, which was left unconstrained with regards to maximum effect size. This relationship was stronger for the increase in CBV (R^2 = 0.98) compared with the decrease in CBV (R^2 = 0.72) but the magnitude of the changes was also larger for the increase in CBV compared with the decrease CBV response.

Spatial distribution of PET and MR signals

As expected, AZ10419369 displaced [^{11}C]AZ10419369 binding uniformly across the brain, with no major differences in the regional 5-HT$_{1B}$R occupancies. Overall, CBV responses were most pronounced in areas with high 5-HT$_{1B}$R binding. However, a few areas, particularly thalamus, putamen, and the vermis, exhibited CBV responses that were pronounced relative to the medium or low regional 5-HT$_{1B}$R binding (Fig. 2).

Effects of the 5-HT$_{1B}$R agonist sumatriptan on the PET-MRI signal

To separately differentiate the hemodynamic effects in brain parenchyma, brain vasculature, and extracranial tissue, we administrated in one animal the less BBB-permeable 5-HT$_{1B}$R agonist sumatriptan. Both sumatriptan (19.4 μg/kg; Fig. 3*A*) and AZ10419369 (36.2 μg/kg; Fig. 3*B*) injections led to extracranial tissue vasoconstriction. The magnitudes of these responses were similar: at the given doses, the peak blood volume change both with sumatriptan and with AZ10419369 was −3.4%. Interestingly, sumatriptan only induced a very small CBV change in putamen but not in any of the other brain regions where AZ10419369 had its major hemodynamic effects (Fig. 3). The simultaneous PET experiments showed that sumatriptan injection was only associated with minor occupancy (~6%) at the 5-HT$_{1B}$R (Fig. 3*C*). For comparison, the dose of AZ10419369 (36.2 μg/kg) that elicited the same degree of vasoconstriction in

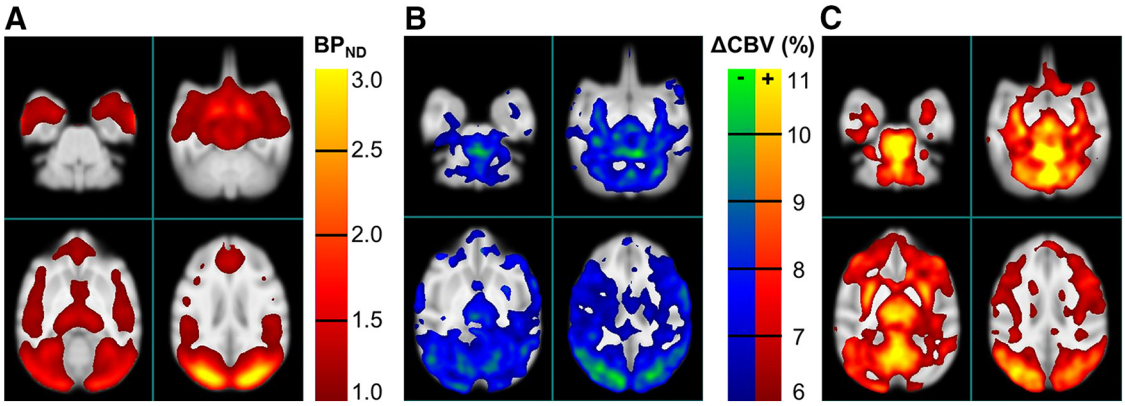

Figure 2. Spatial distribution of PET and MR signals. ***A***, Binding potential map of [^{11}C]AZ10419369 (averaged across 7 scans) and (***B***) negative CBV change and (***C***) positive CBV changes. Images are averages across six experiments with AZ10419369 doses ranging between 0.88 and 5.0 μg/kg. PET data were smoothed with a 3.5 mm Gaussian filter. The *p* value for thresholding of CBV change was $p < 0.001$.

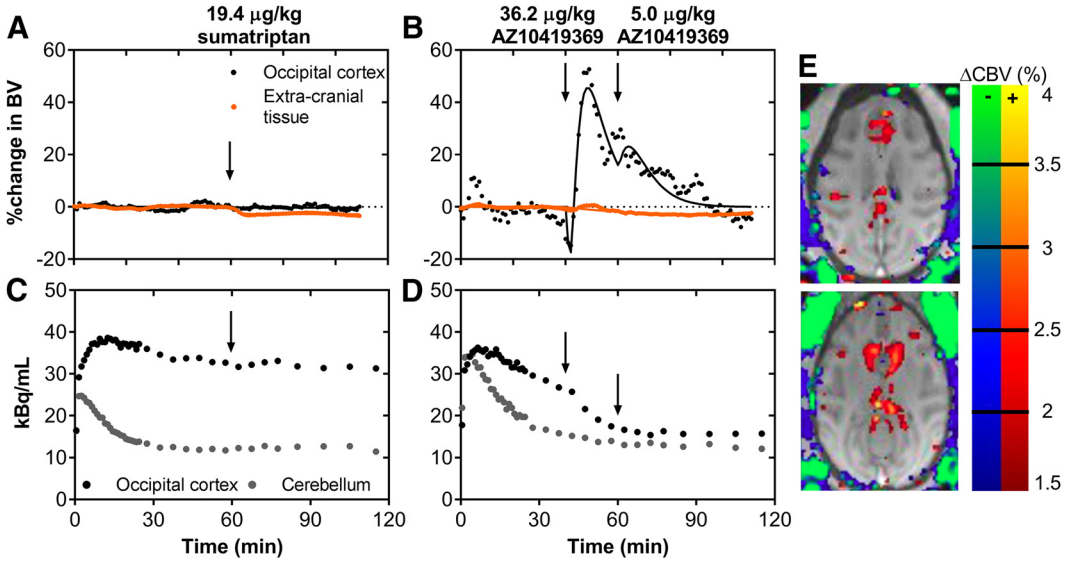

Figure 3. Within-scan challenges of 5-HT$_{1B}$R agonists sumatriptan and AZ10419369. ***A***, CBV changes in the occipital cortex and peripheral tissue in response to the 19.4 μg/kg sumatriptan challenge. ***B***, CBV changes in the occipital cortex and extracranial tissue in response to the 36.2 μg/kg and 5.0 μg/kg AZ10419369 challenges. ***C***, Time-activity curve of [^{11}C]AZ10419369 for the corresponding sumatriptan challenge experiment. ***D***, Time-activity curve [^{11}C]AZ10419369 for the corresponding AZ10419369 challenge experiment. ***E***, Map of blood volume changes in the NHP brain and peripheral tissue in two representative transverse planes. Changes in blue/green colors represent decreases in CBV, whereas changes in yellow/red represent increases in CBV.

extracranial tissue as sumatriptan was associated with a cerebral 5-HT$_{1B}$R occupancy of 69% (Fig. 3*D*).

Together, the dose-dependency of 5-HT$_{1B}$R occupancy, the biphasic hemodynamic response, and the spatial concordance between regional 5-HT$_{1B}$R binding and the magnitude of the hemodynamic response suggested that AZ10419369 elicits its cerebral hemodynamic effects through direct pharmacological action on the parenchymal 5-HT$_{1B}$R and not on the vascular receptors.

The biphasic hemodynamic response is elicited by BBB-permeable agonists but not by antagonists

Next, we examined whether the AZ10419369 dose-dependent hemodynamic effects in the brain parenchyma were elicited by the pharmacological blockade of the 5-HT$_{1B}$R or whether they originated from the agonist properties of AZ10419369. For this purpose, we measured the PET-MR signal after administration of the 5-HT$_{1B}$R antagonist GR127935, which is known to cross the NHP BBB well (Pierson et al., 2008; Nabulsi et al., 2010). An intravenous dose of 200 μg/kg GR127935 ($n = 2$) led to a cerebral 5-HT$_{1B}$R occupancy of ~ 62% (Fig. 4*B*). Although this occupancy is similar to what we saw with the highest dose of AZ10419369, we did not observe a significant change in CBV (Fig. 4*A*). We also confirmed that the 5-HT$_{1B}$R antagonist GR127935 did not elicit vasoconstriction in the extracranial tissue, consistent with its antagonist properties.

Finally, to further verify that the biphasic hemodynamic response is mediated by stimulation of the 5-HT$_{1B}$R, we pretreated the animals with GR127935 (500 μg/kg) before the injection of AZ10419369 (5.0 μg/kg). The substantial blocking of 5-HT$_{1B}$Rs (Fig. 4*D*) prevented the previously seen AZ10419369-induced CBV response (Fig. 4*C*). Of note, none of the pharmacological interventions were associated with any significant changes in the systemic physiology of the NHP (blood pressure, pulse, respiration).

To summarize the effects of the three different drugs used in this study, we looked at the correlation between 5-HT$_{1B}$R occupancy and changes in CBV. With the partial agonist AZ10419369, we found a statistically significant correlation between the 5-HT$_{1B}$R

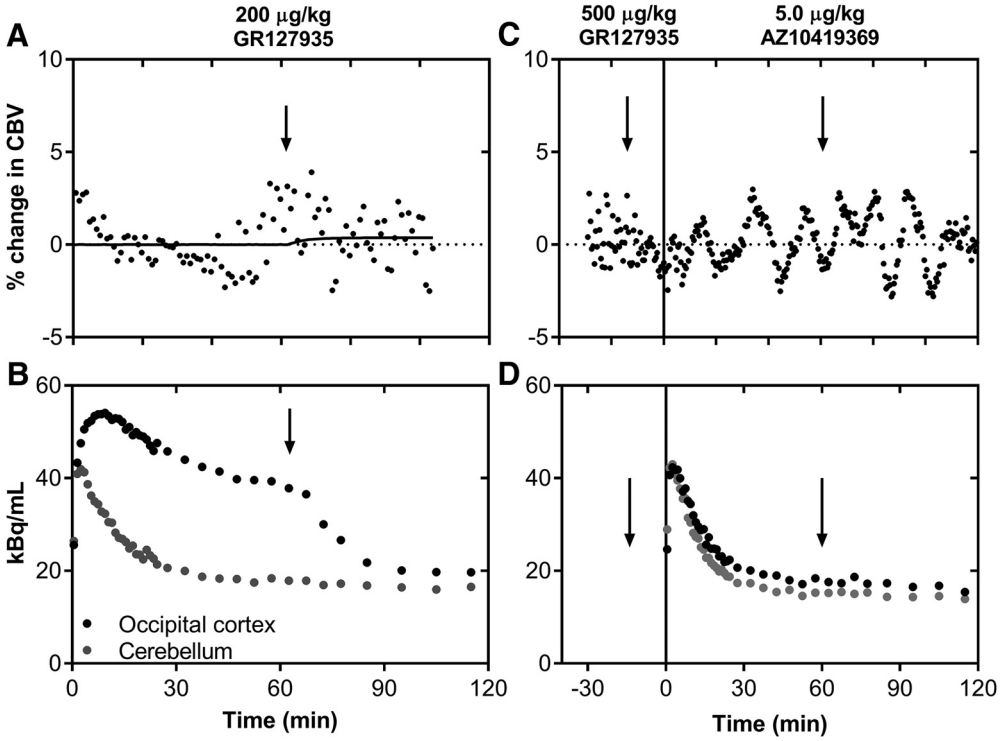

Figure 4. Within-scan challenges and pretreatment with the 5-HT$_{1B}$R antagonist GR127935. ***A***, Average changes in CBV upon administration of GR127935 (200 μg/kg) performed in two different animals. ***B***, Representative time-activity curve of [^{11}C]AZ10419369 with a GR127935 challenge (200 μg/kg). ***C***, Changes in CBV of upon administrating GR127035 (500 μg/kg) before the injection of radioligand and a subsequent within-scan challenge of AZ10419369 (5.0 μg/kg). ***D***, Time-activity curve of [^{11}C]AZ10419369 after GR127935 pretreatment (500 μg/kg) and with a within-scan challenge of AZ10419369.

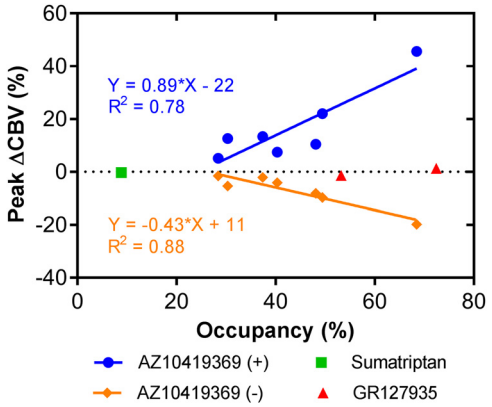

Figure 5. Correlation between the relative changes in 5-HT$_{1B}$R binding and the relative peak changes in CBV in the occipital cortex. The correlation with the decrease in CBV is visualized with orange diamonds, the increase in CBV with blue circles, sumatriptan with a green square, and GR127935 with red triangles. The linear regression of the correlation and the goodness of fit (R^2) are indicated.

receptor occupancy and both the relative decrease ($p = 0.002$, $R^2 = 0.88$) and the increase ($p = 0.009$, $R^2 = 0.78$) in CBV (Fig. 5). By contrast, the antagonist GR127935, which achieved high occupancy, did not show such a relationship. Sumatriptan, because of its low BBB penetrance and consequently low occupancy, did not result in any changes in CBV in the occipital cortex.

Discussion

Here, we demonstrated how simultaneous PET-MR in conjunction with pharmacological interventions can critically inform about spatial and temporal drug actions in the CNS. Using a series of pharmacological probes to study the binding and function of the G-protein-coupled 5-HT$_{1B}$R, unique properties of pharmacological compounds can be identified *in vivo*, including hemodynamic effects in peripheral tissue and in the brain, BBB penetrance and target involvement. Our results confirm that AZ10419369 possesses 5-HT$_{1B}$R agonistic properties. This interpretation is reinforced by (1) data showing that the antagonist GR127935 achieved high receptor occupancy in the absence of a hemodynamic response, consistent with the notion of negligible basal occupancy at this receptor; and (2) comparable extracranial vasoconstriction produced by AZ10419369 and the clinical agonist sumatriptan.

Localization of 5-HT$_{1B}$Rs

Given that cerebral 5-HT$_{1B}$Rs are present both intravascularly (Riad et al., 1998) and as autoreceptors and heteroreceptors (for review, see Sari, 2004)) the central hemodynamic effects could in principle stem from stimulation of 5-HT$_{1B}$Rs in any of these three categories, or a combination thereof. We find it unlikely that the intravascular 5-HT$_{1B}$Rs contribute to the cerebral hemodynamic response because the low-permeable 5-HT$_{1B}$R agonist sumatriptan induced extracranial vasoconstriction as expected (Razzaque et al., 1999) but did not elicit any significant cerebral hemodynamic effects. This is consistent with previous reports on the BOLD effect after administration of sumatriptan (Asghar et al., 2012). Sumatriptan acts in these experiments as a positive control for the agonist action of AZ10419369 outside the BBB. We demonstrated agonism as decreased CBV in extracranial areas as an index of the vasoconstrictive effect of the drugs. In these regions, sumatriptan and AZ10419369 produced similar responses in both magnitude and duration.

Downstream effects of 5-HT$_{1B}$R stimulation

Stimulation of the 5-HT$_{1B}$R with the partial agonist AZ10419369 resulted in a biphasic response with a brief negative CBV response followed by a longer-lasting and larger positive CBV response above baseline. This temporal response can aid interpretation of the underlying pharmacology: the initial fast negative CBV response is consistent with direct 5-HT$_{1B}$R-mediated inhibitory function, through the postsynaptic binding of AZ10419369 at 5-HT$_{1B}$Rs. The changes in CBV can be interpreted in the light of the 5-HT$_{1B}$Rs modulatory role in neurotransmission given the fact that the 5-HT$_{1B}$ heteroreceptor is present on serotonergic, glutamatergic, and particularly on GABAergic neurons throughout the brain (for review, see Sari, 2004). Tanaka and North showed that a 5-HT$_{1B}$R agonist mediate presynaptic inhibition of the EPSPs in layer V of anterior cingulate cortex in rats (Tanaka and North, 1993). Furthermore, a correlation between 5-HT$_{1B}$R and the NMDA receptor binding was recently found in postmortem human tissue using autoradiography (Veldman et al., 2017). Together this support that the decrease in CBV seen in our study is a result of 5-HT$_{1B}$R-mediated decrease in glutamate release. Pharmacological stimulation of 5-HT$_{1B}$ heteroreceptors on GABAergic neurons will result in a reduction in the release of GABA. The net outcome of this disinhibition is excitatory neurotransmission; that is, an increase in metabolism and CBV. Similarly, 5-HT was found to act on presynaptic 5-HT$_{1B}$ heteroreceptors on GABAergic terminals in the ventral midbrain to inhibit the release of GABA on GABA$_B$ receptors (Morikawa et al., 2000). Furthermore, there are data to support that the cerebral GABA concentration can predict the magnitude of negative BOLD responses (Northoff et al., 2007). The biphasic pattern was conserved across the different doses of AZ10419369, and the highest amplitudes were spatially overlapping with highest 5-HT$_{1B}$R densities. This suggests that the size of the regional hemodynamic effects emerges as a combination of receptor density and drug occupancy, in line with previous observations in pharmacological fMRI studies in healthy volunteers (Hornboll et al., 2013). Alternatively, one should also consider whether the functional responses can be downregulated dynamically on a time scale of minutes by desensitization through mechanisms like receptor internalization, as it previously has been demonstrated for the dopaminergic system (Sander et al., 2016). To the best of our knowledge, however, desensitization of the 5-HT$_{1B}$R has not been described.

5-HT$_{1B}$R antagonism

The strength and novelty of the presented data is the use of functionally different compounds, including AZ10419369 as a partial agonist (Maier et al., 2009) and GR127935 as an antagonist (Skingle et al., 1996). Whereas we found a strong positive correlation between the CBV responses and receptor occupancies obtained with AZ10419369, we did not find the same relationship with GR127935, despite the fact that the drugs reached similar occupancies in the brain. According to classical pharmacology, antagonists will occupy the receptors but have zero intrinsic activity, meaning that they do not induce a downstream intracellular effect. Our data with GR127935 fits very well into this model, but only if the occupancy of the endogenous ligand is low and if the receptor is not constitutively active. The observation that GR127935 did not elicit any hemodynamic effect supports the notion that the 5-HT$_{1B}$R endogenous occupancy of 5-HT is low; otherwise, the antagonist-induced reduction in endogenous 5-HT receptor availability would have induced a positive CBV response by displacing neurotransmitter, as is seen with D2 receptor antagonists (Sander et al., 2013). Human 5-HT$_{1B}$Rs display constitutive activity when expressed in recombinant cell systems, and compounds such as methiothepin, SB-224289, and SB-236057-A decrease basal GTPγS activity, indicating that they are inverse agonists (Pauwels et al., 1998; Roberts et al., 2001). However, evidence of these inverse agonist properties has not been confirmed *in vivo* (Roberts et al., 2001; Stenfors and Ross, 2002). Our results also match other studies conducted *in vitro* and *in vivo* that found that although GR127935 itself has little effect, it can block the anti-aggressive effect of 5-HT$_{1B}$R agonists (Doménech et al., 1997; Bannai et al., 2007). As an additional control experiment, we pretreated the animals with a large dose of GR127935 (500 μg/kg) resulting in high 5-HT$_{1B}$R occupancy, and then gave AZ10419369 as a challenge. The outcome confirms that the biphasic hemodynamic response results from 5-HT$_{1B}$R activation and subsequent downstream effects: when virtually no 5-HT$_{1B}$Rs were available for the AZ10419369 challenge, the hemodynamic response was abolished.

Study limitations

A potential limitation of this study is that experiments were conducted in NHP under isoflurane anesthesia to avoid movement and to facilitate the drug interventions. As seen in the dopamine studies performed in the same animals and same PET-MR scanner (Sander et al., 2013), we also observe in some studies large, transient and repetitive changes in fMRI signal that were consistent with isoflurane-induced burst suppression, a noise source that is unlikely to be present in human studies. These burst suppressions caused us to exclude one of the fMRI datasets due to physiological noise. It is known from NHP PET studies that the cerebral GABA$_A$ receptor binding is unaltered in awake and isoflurane anesthetized conditions (Sandiego et al., 2013) supporting that the anesthesia did not directly involve the GABA$_A$ receptors. Anesthesia was in this study induced by ketamine, which in a previous study by Yamanaka et al. (2014) was shown to increase 5-HT$_{1B}$R binding in NHPs. However, in the Yamanaka et al. (2014) study the induction doses were higher (30 mg/kg) than used in the present study (10–20 mg/kg) and furthermore, a continuous infusion of ketamine was applied. In pilot studies reported in the same paper, they did not observe any significant changes in 5-HT$_{1B}$R binding when they gave a dose corresponding to antidepressant dose given to humans, namely 0.75 mg/kg/h.

Perspectives for the use of simultaneous PET-MR

We showed that drugs targeting the 5-HT$_{1B}$R with pharmacologically distinct characteristics elicit specific profiles in the brain's hemodynamic response. We propose that this approach should generalize for testing other systems including, e.g., enzymatic activity or other neurotransmitter systems. Combined simultaneous PET-MRI opens for the possibility of testing novel drug compounds for their BBB passage, their brain occupancy, and their functionality, based upon the hemodynamic response. The G-protein-coupled receptor-effector systems are known to be extraordinarily complex and future drugs might be developed to have bias for distinct effector pathways, a concept coined as functional selectivity. We posit that combined PET-MRI could play a unique role to uncover *in vivo* ligand effects on those effector systems.

The technical advancements can directly be taken to studies in humans and will potently enable acceleration of drug development for brain disorders; an advancement that is highly needed, given the slow progress in the field. We particularly anticipate that the technique will be applied for investigation of novel pharmaceuticals drugs to enable safe testing in humans. The tech-

nique can provide valuable information in any of the clinical trial phases, but it may prove especially useful in Phase 0 where microdosing experiments can be performed. We here show that in low doses (10–30 μg/kg) changes in both the PET and MR signal can be detected. Contrast-enhanced BOLD, as used in this study, greatly improves the sensitivity of the MR signal and is currently being used in humans (D'Arceuil et al., 2013; Baumgartner et al., 2017) but other techniques, such as arterial spin labeling (Wang et al., 2011) can also replace the MR contrast enhancement. The main benefit for CNS drug development is that combined PET-MR imaging can help to effectively assist early decision making in whether to proceed to expensive clinical trials or to await better drug candidates (Nathan et al., 2014).

References

Asghar MS, Hansen AE, Larsson HB, Olesen J, Ashina M (2012) Effect of CGRP and sumatriptan on the BOLD response in visual cortex. J Headache Pain 13:159–166. CrossRef Medline

Bannai M, Fish EW, Faccidomo S, Miczek KA (2007) Anti-aggressive effects of agonists at 5-HT$_{1B}$ receptors in the dorsal raphe nucleus of mice. Psychopharmacology 193:295–304. CrossRef Medline

Baumgartner R, Cho W, Coimbra A, Chen C, Wang Z, Struyk A, Venketasubramanian N, Low M, Gargano C, Zhao F, Williams D, Reese T, Seah S, Feng D, Apreleva S, Petersen E, Evelhoch JL (2017) Evaluation of an fMRI USPIO-based assay in healthy human volunteers. J Magn Reson Imaging 46:124–133. CrossRef Medline

Belliveau JW, Kennedy DN Jr, McKinstry RC, Buchbinder BR, Weisskoff RM, Cohen MS, Vevea JM, Brady TJ, Rosen BR (1991) Functional mapping of the human visual cortex by magnetic resonance imaging. Science 254:716–719. CrossRef Medline

Bourke JH, Wall MB (2015) phMRI: methodological considerations for mitigating potential confounding factors. Front Neurosci 9:167. CrossRef Medline

Catana C, van der Kouwe A, Benner T, Michel CJ, Hamm M, Fenchel M, Fischl B, Rosen B, Schmand M, Sorensen AG (2010) Toward implementing an MRI-based PET attenuation-correction method for neurologic studies on the MR-PET brain prototype. J Nucl Med 51:1431–1438. CrossRef Medline

Catana C, Drzezga A, Heiss WD, Rosen BR (2012) PET/MRI for neurologic applications. J Nucl Med 53:1916–1925. CrossRef Medline

da Cunha-Bang S, Hjordt LV, Perfalk E, Beliveau V, Bock C, Lehel S, Thomsen C, Sestoft D, Svarer C, Moos Knudsen GM (2017) Serotonin 1B receptor binding is associated with trait anger and level of psychopathy in violent offenders. Biol Psychiatry 82:267–274. CrossRef Medline

D'Arceuil H, Coimbra A, Triano P, Dougherty M, Mello J, Moseley M, Glover G, Lansberg M, Blankenberg F (2013) Ferumoxytol enhanced resting state fMRI and relative cerebral blood volume mapping in normal human brain. Neuroimage 83:200–209. CrossRef Medline

Doménech T, Beleta J, Palacios JM (1997) Characterization of human serotonin 1D and 1B receptors using [^{3}H]-GR-125743, a novel radiolabelled serotonin 5HT1D/1B receptor antagonist. Naunyn Schmiedebergs Arch Pharmacol 356:328–334. CrossRef Medline

Elhusseiny A, Hamel E (2001) Sumatriptan elicits both constriction and dilation in human and bovine brain intracortical arterioles. Br J Pharmacol 132:55–62. CrossRef Medline

Geyer MA (1996) Serotonergic functions in arousal and motor activity. Behav Brain Res 73:31–35. Medline

Hornboll B, Macoveanu J, Rowe J, Elliott R, Paulson OB, Siebner HR, Knudsen GM (2013) Acute serotonin 2A receptor blocking alters the processing of fearful faces in the orbitofrontal cortex and amygdala. J Psychopharmacol 27:903–914. CrossRef Medline

Jenkins BG (2012) Pharmacologic magnetic resonance imaging (phMRI): imaging drug action in the brain. Neuroimage 62:1072–1085. CrossRef Medline

Lindsley CW (2014) New statistics on the cost of new drug development and the trouble with CNS drugs. ACS Chem Neurosci 5:1142. CrossRef Medline

Maier DL, Sobotka-Briner C, Ding M, Powell ME, Jiang Q, Hill G, Heys JR, Elmore CS, Pierson ME, Mrzljak L (2009) [*N*-methyl-^{3}H$_3$]AZ10419369 binding to the 5-HT1$_B$ receptor: *in vitro* characterization and *in vivo* receptor occupancy. J Pharmacol Exp Ther 330:342–351. CrossRef Medline

Mandeville JB (2012) IRON fMRI measurements of CBV and implications for BOLD signal. Neuroimage 62:1000–1008. CrossRef Medline

Mandeville JB, Marota JJ, Kosofsky BE, Keltner JR, Weissleder R, Rosen BR, Weisskoff RM (1998) Dynamic functional imaging of relative cerebral blood volume during rat forepaw stimulation. Magn Reson Med 39:615–624. CrossRef Medline

Matthews PM, Rabiner EA, Passchier J, Gunn RN (2012) Positron emission tomography molecular imaging for drug development. Br J Clin Pharmacol 73:175–186. CrossRef Medline

Morikawa H, Manzoni OJ, Crabbe JC, Williams JT (2000) Regulation of central synaptic transmission by 5-HT$_{1B}$ auto- and heteroreceptors. Mol Pharmacol 58:1271–1278. CrossRef Medline

Nabulsi N, Huang Y, Weinzimmer D, Ropchan J, Frost JJ, McCarthy T, Carson RE, Ding YS (2010) High-resolution imaging of brain 5-HT$_{1B}$ receptors in the rhesus monkey using [^{11}C]P943. Nucl Med Biol 37:205–214. CrossRef Medline

Nathan PJ, Phan KL, Harmer CJ, Mehta MA, Bullmore ET (2014) Increasing pharmacological knowledge about human neurological and psychiatric disorders through functional neuroimaging and its application in drug discovery. Curr Opin Pharmacol 14:54–61. CrossRef Medline

Nord M, Cselenyi Z, Forsberg A, Rosenqvist G, Tiger M, Lundberg J, Varrone A, Farde L (2014) Distinct regional age effects on [^{11}C]AZ10419369 binding to 5-HT$_{1B}$ receptors in the human brain. Neuroimage 103:303–308. CrossRef Medline

Northoff G, Walter M, Schulte RF, Beck J, Dydak U, Henning A, Boeker H, Grimm S, Boesiger P (2007) GABA concentrations in the human anterior cingulate cortex predict negative BOLD responses in fMRI. Nat Neurosci 10:1515–1517. CrossRef Medline

Pauwels PJ, Wurch T, Palmier C, Colpaert FC (1998) Pharmacological analysis of G-protein activation mediated by guinea-pig recombinant 5-HT$_{1B}$ receptors in C6-glial cells: similarities with the human 5-HT$_{1B}$ receptor. Br J Pharmacol 123:51–62. CrossRef Medline

Pierson ME, Andersson J, Nyberg S, McCarthy DJ, Finnema SJ, Varnäs K, Takano A, Karlsson P, Gulyás B, Medd AM, Lee CM, Powell ME, Heys JR, Potts W, Seneca N, Mrzljak L, Farde L, Halldin C (2008) [^{11}C]AZ10419369: a selective 5-HT$_{1B}$ receptor radioligand suitable for positron emission tomography (PET). Characterization in the primate brain. Neuroimage 41:1075–1085. CrossRef Medline

Qiu D, Zaharchuk G, Christen T, Ni WW, Moseley ME (2012) Contrast-enhanced functional blood volume imaging (CE-fBVI): enhanced sensitivity for brain activation in humans using the ultrasmall superparamagnetic iron oxide agent ferumoxytol. Neuroimage 62:1726–1731. CrossRef Medline

Razzaque Z, Heald MA, Pickard JD, Maskell L, Beer MS, Hill RG, Longmore J (1999) Vasoconstriction in human isolated middle meningeal arteries: determining the contribution of 5-HT$_{1B}$- and 5-HT$_{1F}$-receptor activation. Br J Clin Pharmacol 47:75–82. CrossRef Medline

Riad M, Tong XK, el Mestikawy S, Hamon M, Hamel E, Descarries L (1998) Endothelial expression of the 5-hydroxytryptamine 1B antimigraine drug receptor in rat and human brain microvessels. Neuroscience 86:1031–1035. CrossRef Medline

Roberts C, Watson J, Price GW, Middlemiss DN (2001) SB-236057-A: a selective 5-HT1B receptor inverse agonist. CNS Drug Rev 7:433–444. CrossRef Medline

Ruf BM, Bhagwagar Z (2009) The 5-HT1B receptor: a novel target for the pathophysiology of depression. Curr Drug Targets 10:1118–1138. CrossRef Medline

Sander CY, Hooker JM, Catana C, Normandin MD, Alpert NM, Knudsen GM, Vanduffel W, Rosen BR, Mandeville JB (2013) Neurovascular coupling to D2/D3 dopamine receptor occupancy using simultaneous PET/functional MRI. Proc Natl Acad Sci U S A 110:11169–11174. CrossRef Medline

Sander CY, Hooker JM, Catana C, Rosen BR, Mandeville JB (2016) Imaging agonist-induced D2/D3 receptor desensitization and internalization *in vivo* with PET/fMRI. Neuropsychopharmacology 41:1427–1436. CrossRef Medline

Sandiego CM, Jin X, Mulnix T, Fowles K, Labaree D, Ropchan J, Huang Y, Cosgrove K, Castner SA, Williams GV, Wells L, Rabiner EA, Carson RE (2013) Awake nonhuman primate brain PET imaging with minimal head restraint: evaluation of GABA$_A$-benzodiazepine binding with ^{11}C-flumazenil in awake and anesthetized animals. J Nucl Med 54:1962–1968. CrossRef Medline

Sari Y (2004) Serotonin 1B receptors: from protein to physiological function and behavior. Neurosci Biobehav Rev 28:565–582. CrossRef Medline

Schoeffter P, Hoyer D (1989) How selective is GR43175? Interactions with functional 5-HT1B, 5-HT1C and 5-HT1D receptors. Naunyn Schmiedebergs Arch Pharmacol 340:135–138. Medline

Schytz HW, Hargreaves R, Ashina M (2017) Challenges in developing drugs for primary headaches. Prog Neurobiol 152:70–88. CrossRef Medline

Skingle M, Beattie DT, Scopes DI, Starkey SJ, Connor HE, Feniuk W, Tyers MB (1996) GR127925: a potent and selective 5-HT1D receptor antagonist. Behav Brain Res 73:157–161. Medline

Stenfors C, Ross SB (2002) Failure to detect *in vivo* inverse agonism of the 5-HT1B receptor antagonist SB-224289 in 5-HT-depleted guinea-pigs. Naunyn Schmiedebergs Arch Pharmacol 365:462–467. CrossRef Medline

Tanaka E, North RA (1993) Cocaine enhancement of the action of 5-hydroxytryptamine in rat cingulate cortex *in vitro*. Neurosci Lett 163: 50–52. CrossRef Medline

Veldman ER, Svedberg MM, Svenningsson P, Lundberg J (2017) Distribution and levels of 5-HT 1B receptors in anterior cingulate cortex of patients with bipolar disorder, major depressive disorder and schizophrenia: an autoradiography study. Eur Neuropsychopharmacol 27:504–514. CrossRef Medline

Wang DJ, Chen Y, Fernández-Seara MA, Detre JA (2011) Potentials and challenges for arterial spin labeling in pharmacological magnetic resonance imaging. J Pharmacol Exp Ther 337:359–366. CrossRef Medline

Yamanaka H, Yokoyama C, Mizuma H, Kurai S, Finnema SJ, Halldin C, Doi H, Onoe H (2014) A possible mechanism of the nucleus accumbens and ventral pallidum 5-HT1B receptors underlying the antidepressant action of ketamine: a PET study with macaques. Transl Psychiatry 4:e342. CrossRef Medline

Zhou Y, Chen MK, Endres CJ, Ye W, Brasić JR, Alexander M, Crabb AH, Guilarte TR, Wong DF (2006) An extended simplified reference tissue model for the quantification of dynamic PET with amphetamine challenge. Neuroimage 33:550–563. CrossRef Medline